Neurocomputing 557 (2023) 126710

Contents lists available at ScienceDirect

Neurocomputing

journal homepage: www.elsevier.com/locate/neucom

Learning in colloids: Synapse-like ZnO + DMSO colloid

Noushin Raeisi Kheirabadi [a,*], Alessandro Chiolerio [b,a], Neil Phillips [a], Andrew Adamatzky [a]

[a] Unconventional Computing Laboratory, University of the West of England, Bristol, UK
[b] Center for Bioinspired Soft Robotics, Istituto Italiano di Tecnologia, Genova, Italy

ARTICLE INFO

Keywords:
Neuromorphic device
Colloid
Memory devices
Artificial synapse
Liquid computing
Liquid robotics

ABSTRACT

Colloids subjected to electrical stimuli exhibit a reconfiguration that might be used to store information and potentially compute. In a colloidal suspension of ZnO nanoparticles in DMSO, we investigated the learning, memorization, time and stimulation's voltage dependence of conductive network formation. The relationships between the critical resistance and stimulation time have been reconstructed. The critical voltage (i.e., the stimulation voltage required to drop the resistance) was found to decrease as stimulation time increased. We characterized a dispersion of conductive ZnO nanoparticles in the DMSO polymeric matrix using FESEM and UV–visible absorption spectrum.

1. Introduction

Colloids could be used to implement massively parallel computations given that they possess a wide variety of unique properties. The particles are stable, so they remain suspended in the solution. Therefore, in a colloid processor, any particle can be addressed to access a memory cell [1]. Moreover, due to the redundancy of the elementary processors, or particles, colloid computers could be fault-tolerant.

A colloid of conductive particles in an insulating solution is a strong candidate for colloid-based computers. In this paper, zinc oxide particles are suspended in a polymer dimethyl sulfoxide solution. Polymers in their natural state (with some exceptions) are insulating materials [2], and modulating their electrical conductivity, regardless of application, requires blending with materials exhibiting electronic/ionic conductivity. Fillers in the metallic state, for instance, permit increased electronic conduction and, depending on their shape and aspect ratio, may create a complete network that provides a preferential route for charge carriers. Silver nanoparticles/nanowires [3] are frequently used as conductive fillers and serve as an example. The metallic state can be achieved in part by carbon-based materials, allowing for a good balance in terms of the availability of raw materials. Examples include graphene, carbon fibres, and carbon nanotubes that exceed a threshold concentration in a common polymer [4]. The concentration above which percolation occurs (U) is known as the critical concentration [5–7]. Percolation occurs following a phase transition in which a dramatic change occurs at a single sharply defined parameter value as the concentration is continuously altered [8,9]. Reducing the percolation threshold of a composite system appears to be an effective strategy for reducing the amount of (precious) filler required to achieve the desired conductivity and thereby avoiding mechanical performance issues [10].

Attempts to employ alternative percolation models to describe conductive polymer composites have demonstrated that no single model can explain all of the experimentally observed results [11]. The discrepancy could be related to the fact that conductivity is highly dependent on the geometric parameters of the filler, the quality of their bonds, and the matrix-filler interaction [6,12]. Until now, the majority of research on the dynamic process of conductive network generation in an electric field focused on composites containing conductive fillers such as carbon black (CB), carbon fibres (CF), or carbon nanotubes (CNT) [13,14]. However, and this is a fundamental aspect of our research, there is no simple way to alter conduction properties once a composite material has been formed and given its physical form. Having an easily-tunable material would allow us to create switches, memories, and other computing-essential devices. Chemical reactions involving different oxidation states may also be exploited when triggered by high electric fields. However, activation energies must be overcome and specific fabrication conditions must be met, so applications are not straightforward [15,16].

Nanofluids, or colloidal dispersion of nanoparticles in a liquid solvent, have attracted a great deal of interest in recent years due to their potential applications [17], which include intrinsic plasticity, self-adaptation, and fault-tolerance [18,19]. A stable colloid is expected to remain sediment-free even after lengthy periods of storage [18,19]. The settling behaviour of dispersions is determined by the particle size and density. Nanopowder liquid dispersion is a challenging process. Nanomaterials' favourable effects are a result of their high surface area and surface energy, which cause particle agglomeration and poor-quality dispersions.

* Corresponding author.
E-mail address: Noushin.Raeisikheirabadi@uwe.ac.uk (N.R. Kheirabadi).

https://doi.org/10.1016/j.neucom.2023.126710
Received 3 November 2022; Received in revised form 11 May 2023; Accepted 15 August 2023
Available online 19 August 2023

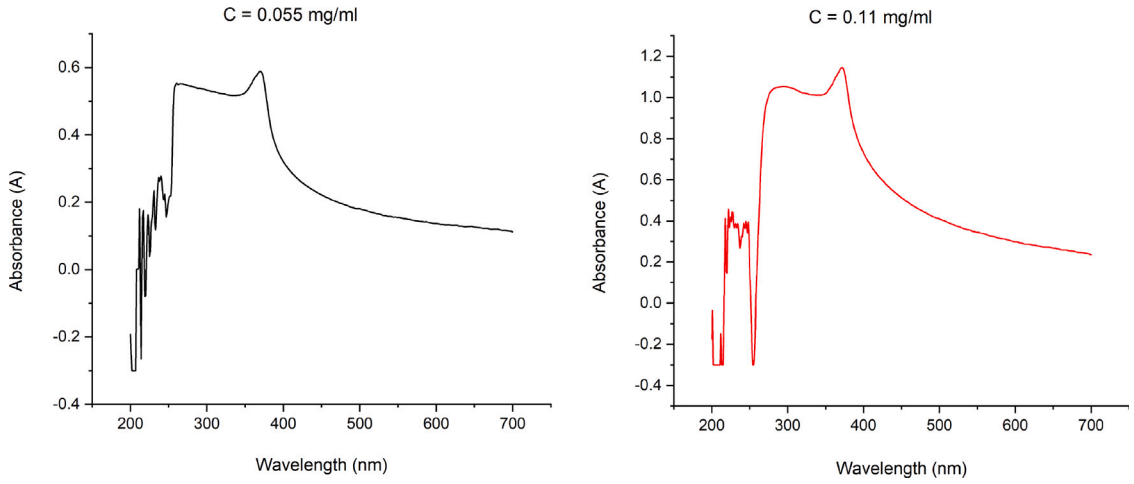

Fig. 1. UV–Visible spectra of the sample with concentrations 0.055 and 0.11 mg/ml.

Due to their fascinating novel optical and electrical properties, research on quantum-sized semiconductor particles has exploded over the past decade [20]. ZnO is a semiconducting material with a wide band gap and a high exciton binding energy of 60 meV at room temperature, making it an appealing candidate for room temperature UV lasers and other fascinating excited-state phenomena [21,22]. ZnO is a versatile material with high electrical conductivity, visual transparency, photostability, and photocatalytic abilities [23,24].

As predicted by classical percolation theory for a random system [25,26], the percolation threshold for simple binary composites is between 10% up to 70%, depending entirely on the aspect ratio of the filler. Once a percolation threshold has been reached, random resistor networks typically exhibit a power-law conductivity relationship.

$$\sigma = \sigma_0(V - V_c)^s$$

where σ is the composite conductivity (S/cm), σ_0 is the intrinsic conductivity of the filler, s is the power-law exponent (typically 1.6–2.0 in 3D), and V_c is the volume fraction of filler at the percolation threshold (near 0.15 for random fibre-based 3D systems) [27].

Von Neumann computer architecture (in which the memory and CPU are separated) only permits instructions to be executed sequentially and one at a time, thereby limiting parallel operations [28]. It is anticipated that the next generation of computing systems will use synthetic synapses (which mimic biological synapses) to enable parallel processing of information [29]. Resistive switching and synaptic properties of learning colloids could theoretically be employed to enable massively parallel computing [30,31].

Using ZnO nanoparticles dissolved in DMSO, the purpose of the present study is to create highly mobile ion-conductive pathways. It is expected that the free migration of ions will result in high ionic conductivity. We investigate how, using a filler with spherical symmetry and a 3D composite fluid, a percolation threshold can be achieved at low concentrations.

2. Methods

ZnO nanoparticles and DMSO were purchased from US research nanomaterials, Sodium Dodecyl Sulphate (SDS) and Sodium Hydroxide (NaOH) were purchased from Merck. De-Ionized Water (DIW) were prepared in the lab with Millipore de-ionized water generator device, model Essential, rated 15 Mohm cm.

Surfactant solution with a concentration of 0.22 wt% was prepared by adding SDS in DIW and stirred to get a homogeneous solution. 1 mg ZnO nanoparticles were added to DMSO with continuous stirring. Then 2 ml of SDS solution and 1 ml NaOH 10M added to the mixture under stirring. The concentration of resulting dispersion was maintained at 0.11 mg/ml. The resulted suspension was placed in an ultrasonic bath for 30 min. Then stirring process was continued for a few more hours to get a uniform dispersion of ZnO [32].

All electrical measurements were made with Fluke 88464A and Keithley 2400. Field emission scanning Electron Microscopy (FEI Quanta 650 FESEM) was also used to characterize the nanoparticle suspensions. The accelerating voltage was set to 10 kV in this study, and the working distance was set to around 5 mm. The images' contrast and brightness were optimized so that particles could be easily distinguished from the background. Ultraviolet–visible (UV–Vis.) spectrometer (Perkin Elmer Lambda XLS) was used to measure sample absorbance at room temperature. To analyse the z-average hydrodynamic diameter, Dynamic Light Scattering (DLS) measurements were performed using a Zetasizer Nano ZS (1000 HS, Malvern Instrument Ltd., UK).

3. Results and discussions

3.1. Suspension structure

The UV–visible absorption spectrum of ZnO colloids, with different concentration, at room temperature is recorded in the wavelength range of 200–700 nm. Fig. 1 depicts resulted plots of UV–visible absorption spectrum. The spectra have peaks at 370 nm (colloid with concentration of 0.055 mg/ml) and 372 nm (colloid with concentration of 0.11 mg/ml). These absorption peaks at 370–372 nm are the characteristic peak for hexagonal ZnO nanoparticles [33]. In comparison to bulk ZnO (370 nm), there is a good agreement with previous reports [34,35]. Calculation of the optical band gap was based on the below equation:

$$E_g(\text{eV}) = hc/\lambda = 1240/\lambda$$

where E_g is the optical band gap, h is the Planck's constant, c is the speed of light, and λ is the wavelength of maximum absorption. Here Optical band gap was calculated as 3.35 eV which matches well with previous reports [34,36,37].

In order to study particles morphology and size by FESEM technique, a thin layer of ZnO colloid were prepared by drop casting a drop of ZnO particle suspension (0.11 mg/ml) on a Copper foil with a thickness of 100 μm at room temperature.

FESEM results in Fig. 2 illustrates particle agglomeration during sample preparation. As a result of the surface tension of the solvent during evaporation, FESEM observation rarely reveals separated spheres, and most of the ZnO spheres are multilayered. Indeed, increased liquid surface tension would draw the nanoparticles closer together, causing them to re-aggregate during the drying process [38]. However, we

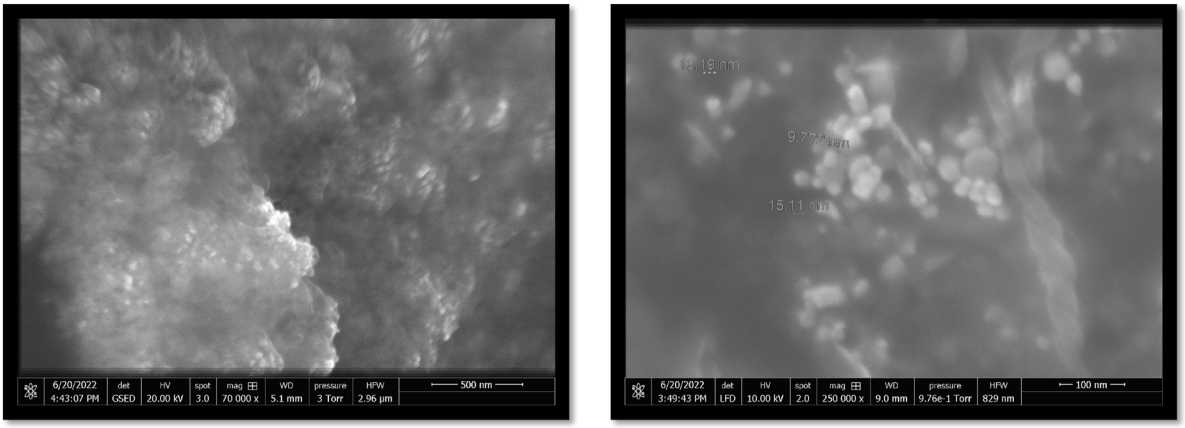

Fig. 2. SEM images of drop casted ZnO colloids on Copper substrate in two different magnifications.

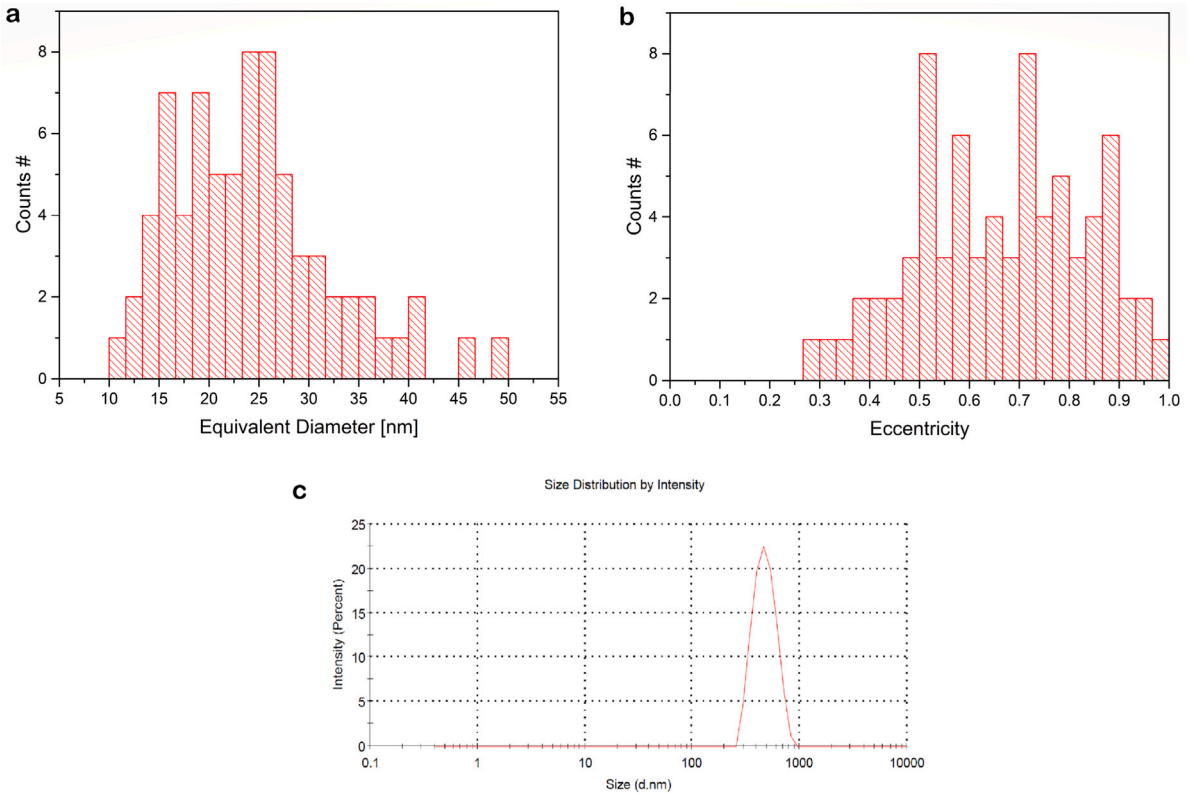

Fig. 3. (a) Equivalent diameter size distribution of ZnO nanoparticle. (b) Numerical eccentricity distribution of ZnO nanoparticles. (c) Particle size distribution of ZnO nanoparticles in colloidal solution using dynamic light scattering.

could extract equivalent diameter size distribution of the single particles, whose histogram is shown in Fig. 3(a), as well as the numerical eccentricity distribution, shown in Fig. 3(b) (numerical eccentricity is zero for a circular nanoparticle and unitary for a nanowire). Relevant features detected are: mean diameter 24 nm, standard deviation 8 nm, skewness 0.874, Kurtosis 0.856, minimum diameter detected 10 nm, maximum diameter detected 50 nm.

Dynamic Light Scattering (DLS) characterization was performed, and Fig. 3(c) indicates the size distribution of ZnO nanoparticles present in the colloid. The average gyration (hydrodynamic) diameter of a particle is 472 nm, and this corresponds almost perfectly to 20 times the average diameter of one single particle. As an amphoteric oxide, ZnO is hydrolysed in the presence of water creating a hydroxide coating on its surface, which leads to an increase in particle hydrodynamic diameter [39].

3.2. Suspension conductivity

To study a formation of conductive network of nanoparticles we carried out DC stimulation of the suspension mixture with different parameters of the stimulation. Fig. 4 illustrates a schematic related to conducted research.

In the first step, DC stimulation versus time at the rate of 10 mV/s from 0 V to 40 V, with Keithley, have been applied to the sample and current was measured. Results are shown in Fig. 5(a). The increase in voltage, resulting in a decrease in resistance. So the first step experiment is: (1) apply voltage growing from 0 to 40, (2) measure resistance, (3) Repeat.

To check the repeatability of this result, DC stimulation has been applied from 0 V to 40 V, with Keithley, to the sample for 10 times and then current was measured. All data are integrated in the Fig. 5(b–c).

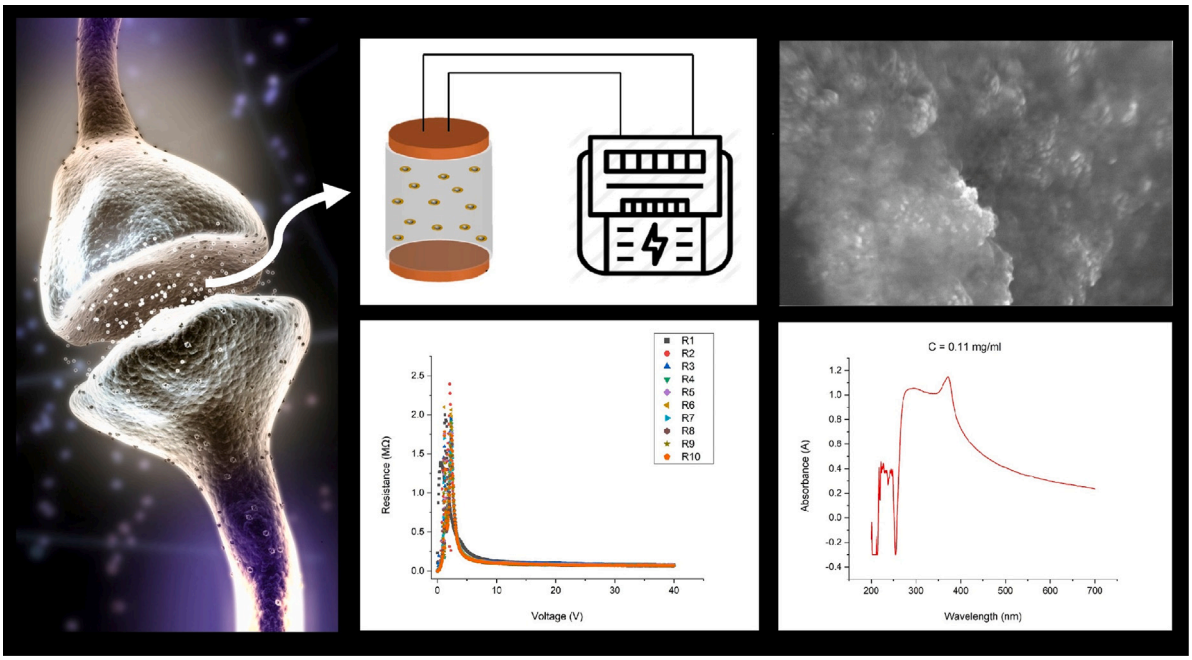

Fig. 4. Schematic of conducted research by synthesized colloid and its characteristic properties.

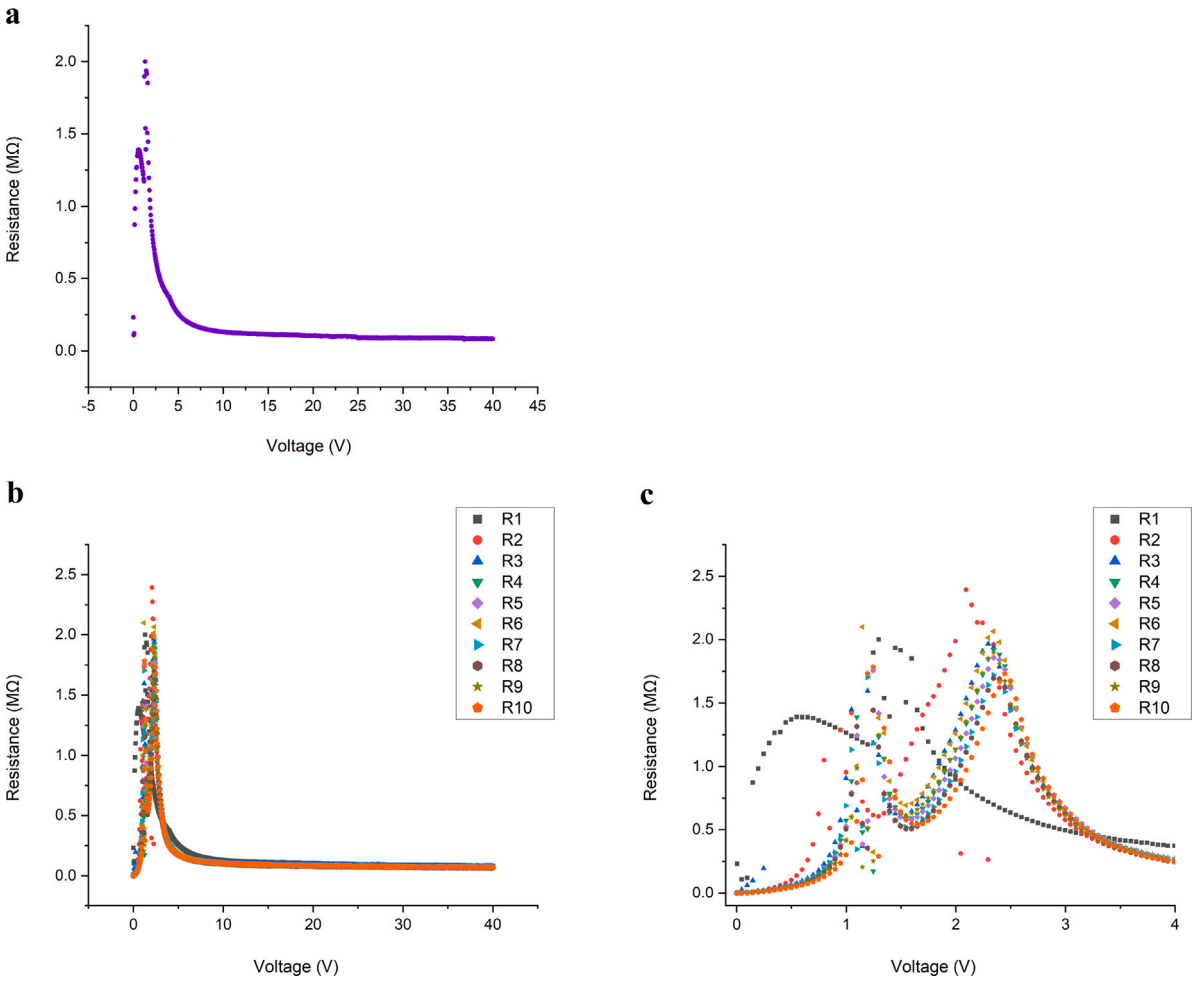

Fig. 5. (a) Resistance diagram of colloid after 40 V DC stimulation, (b) Repeated measurement resistance of colloid with stimulation till 40 V, (c) plot section b with zoom on the first area of the curve.

Table 1
Relation between the length of stimulation, critical voltage and resistance dropping point.

Each stimulus duration (ms)	Time of dropping R (s)	Stimulation length (s)	Highest R (MΩ)	Critical voltage (V)	Critical resistance (MΩ)
1	1	10	1.21	1.55	1.21
10	5	13	1.38	1.45	1.38
100	8	22	1.37	1.40	1.37
1000	22	111	1.76	0.95	1.76
2000	29	211	2.83	0.65	2.83
3000	49	312	3.96	0.75	3.96
4000	63	412	3.18	0.75	3.18

Table 2
The equation and parameters of fitting curve of critical voltage versus length of stimulation.

Equation	Parameter, *a*	Parameter, *b*	Parameter, c	R-Square (COD)
$y = exp(a + bx + cx^2)$	0.470 ± 0.028	−0.006 ± 6.61E^{-4}	1.02E^{-5} ± 1.71E^{-6}	0.98

Table 3
The equation and parameters of fitting curve of critical resistance versus length of stimulation.

Equation	Parameter, y−0	Parameter, x_c	Parameter, W	Parameter, A	R-Square (COD)
y = y − 0 + A sin(pi(x − x_c)/w)	2.56 ± 0.068	180.51 ± 8.33	281.40 ± 18.14	1.28 ± 0.092	0.99

Table 4
The equation and parameters of fitting curve of time of dropping resistance VS length of stimulation.

Equation	Intercept, a	slope, b	R-Square (COD)
y = a + bx	2.64 ± 1.64	0.14 ± 0.008	0.99

Fig. 5(b) shows the repeated measurement resistance of sample with stimulation till 40 V and Fig. 5(c) shows the same plot with zoom on the first area of the curve. Just the first stimulation has a little different resistance curve in comparison with the other 9 stimulations, as it often occurs in similar systems such as resistive switching devices. An interesting feature is the presence of maximum resistance, found in the range of 2 to 2.5 V and then it drops down. As bubbling was observed during apply voltage, probably from 2 V till 3 V, bubbling accrues and misses the order of nanoparticles so R increases. Perhaps after 3 V, the voltage is enough strong to overcome bubbling turbulence and reorder nanoparticles again so R decreases again.

In the second step, the minimum stimulation voltage for a resistance to drop were investigated. In this regard, 5 V, 4 V and 3 V DC stimulation were applied to the sample and then the resistance was measured. Fig. 6 indicates the resistance change during the voltage rising. In all three graphs, the resistance starts to drop down at a voltage of about 0.7 V and it decreases from ~7 MΩ to ~78 kΩ.

For conductive particles filled polymer composites, the percolation hypothesis is commonly employed to describe the sharp change in electrical resistivity as a function of filler content [8]. However, in our case, the filler content has been fixed. To distinguish the link between electrical resistivity and stimulation voltage and during of stimulation, from the filler concentration dependence of percolation, we refer to the stimulation dependence of percolation process as 'percolation time'. To discover the relation between duration of stimulation, critical voltage (a value of voltage at which the resistance starts to decrease) and resistance dropping point, the sample has been stimulated with several times and the resistance was measured in each step. All data are summarized in Table 1.

Fig. 7(a) shows the relation between critical voltage with length of stimulation. Critical voltage decrease with increase in stimulation length. The equation and parameters of fitting its curve are summarized in the Table 2.

Fig. 7(b) shows the relation between critical resistance with length of stimulation. Critical resistance rises with increase in stimulation length till reaches the amount of 3.96 MΩ and then with more enhancement in stimulation length, it falls again. The equation and parameters of fitting this curve are summarized in the Table 3.

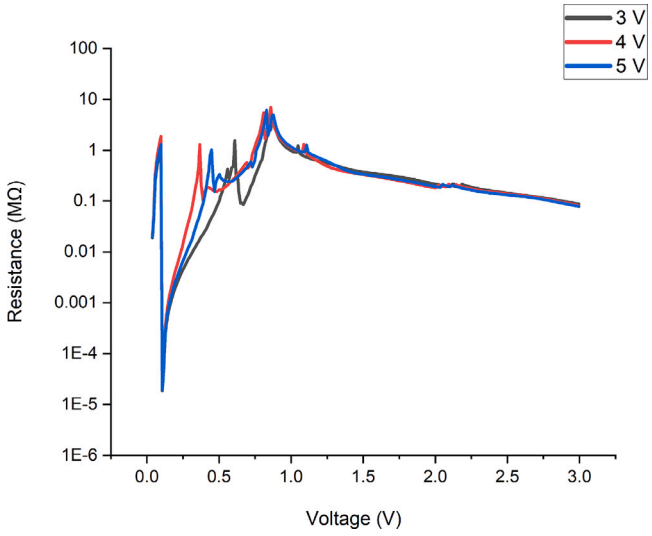

Fig. 6. Finding minimum voltage: Resistance of colloid with stimulation till 3 V, 4 V, and 5 V. There is a Fuchsian discontinuity that is cancelled by the modulus.

The filled conductive colloid are discovered to be thermodynamically non-equilibrium systems, in which the conductive network generation is time dependent, leading to the development of a concept known as dynamic percolation [8]. In this research, the time of dropping resistance depends on the length of stimulation, linearly. This relation is shown in Fig. 7(c) and the fitting parameters are presented in Table 4.

Electrical resistance before and after stimulation were compared to quantify both the quality and duration of the memory. To check the memorization process, the resistance behaviour before and after stimulation, and find for how long does the stimulation effects last, some experiments were implemented. Firstly, the resistance of sample was measured without any stimulation other than the 400 μV applied by the measuring device, and then after applying DC stimulation, from 0 V to 10 V, the resistance was measured again continuously (Fig. 8,a), to find the stability of the dropped resistance. Secondly, the stimulated sample

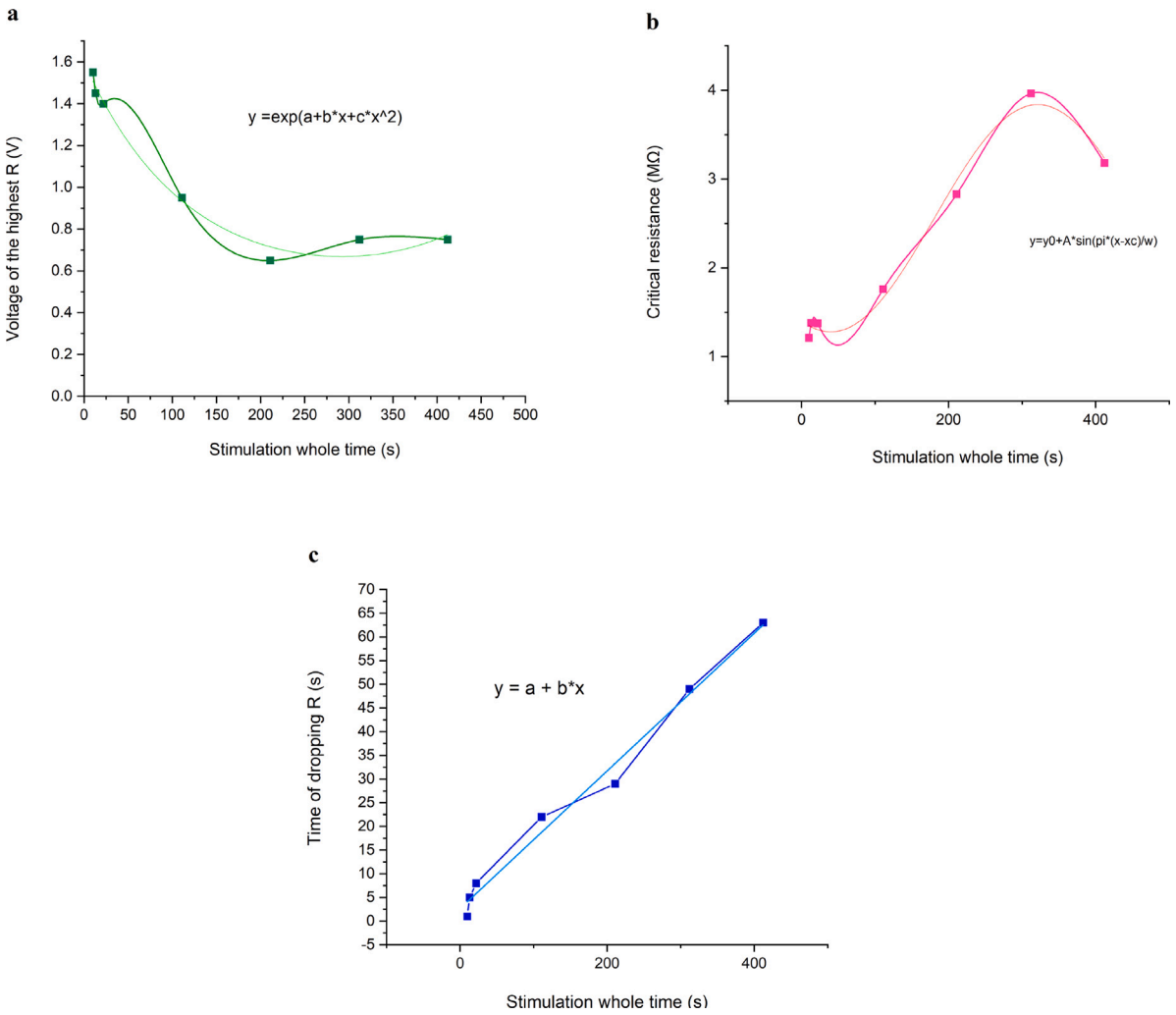

Fig. 7. (a) Relation between critical voltage and length of stimulation, (b) Relation between critical resistance and length of stimulation, (c) Relation between length of stimulation and the time of dropping resistance.

was placed without any moving and any further stimulation. Then its resistance was measured just after stopping stimulation (Fig. 8,b), after 1 h, 2.5 h, 24 h, 48 h and 120 h. All results are shown in the Fig. 8(c).

Resistance was about 1.3 MΩ before applying any stimulation, during applying 10 V DC stimulation, resistance dropped down to under ~ 1 kΩ (Fig. 8,a). After stopping stimulation, the resistance started to rise from under 1 kΩ to 6.5 kΩ by spending 30 min (Fig. 8,b). In one hour, the resistance increased to 96 kΩ, in 2.5 h to 128 kΩ, in 24 h to 370 kΩ, and in 120 h to 600 kΩ (Fig. 8,c). As it can be seen, the resistance increases slowly during 120 h after stopping stimulation indicating memory existence in our colloid.

In order to study the reverse cycle, the switching of the resistance back from low R to high R by reversing voltage were investigated. In the first stage, DC stimulation from 0 V to 10 V, were applied with Keithley to the sample and then the resistance was measured. In the next stage, this process was repeated but in reverse cycle (applying DC stimulation from 10 V to 0 V). Fig. 9(a–b) indicate the current diagram and the resistance diagram of this test, respectively.

In the next step, the polarity of electrodes was changed. The sample have been stimulated from 0 V to 50 V with direct polarity, first. Then the cables on Keithley ports were swapped (without moving electrodes) and sample have been stimulated again from 0 V to 50 V but with indirect polarity. The resulted current and resistance diagrams are shown in the Fig. 9(c–d), respectively. The hysteresis loop of current and voltage shown in Fig. 9(c) indicates history is more prominent in voltage and current approach zero.

Multiple cycles of 'learning-erasing', direct-inverse cycles of stimulation, were repeated in order to evaluate the durability of the colloid device and its results are shown in Fig. 10. The diagram indicates that the results are still consistent, which demonstrates the durability of the colloid device.

Finally, to check the effects of Brownian movements and oxygen interactions, we repeated the DC stimulation experiments under Nitrogen gas and at 12 °C. This test was repeated four times. Fig. 11 shows the results of this experiment and compares them with the previous tests in an ambient atmosphere. No significant differences are observed between these two atmospheric conditions. Hence, we can conclude that Brownian movements and oxygen interactions do not have obvious effects on the learning and memorization process of the synthesized colloid.

4. Conclusion

We demonstrated that a colloid of zinc oxide in dimethyl sulfoxide is capable of forming conducting pathways when a direct current is applied. The conductivity pathways are volatile; they degraded over time.

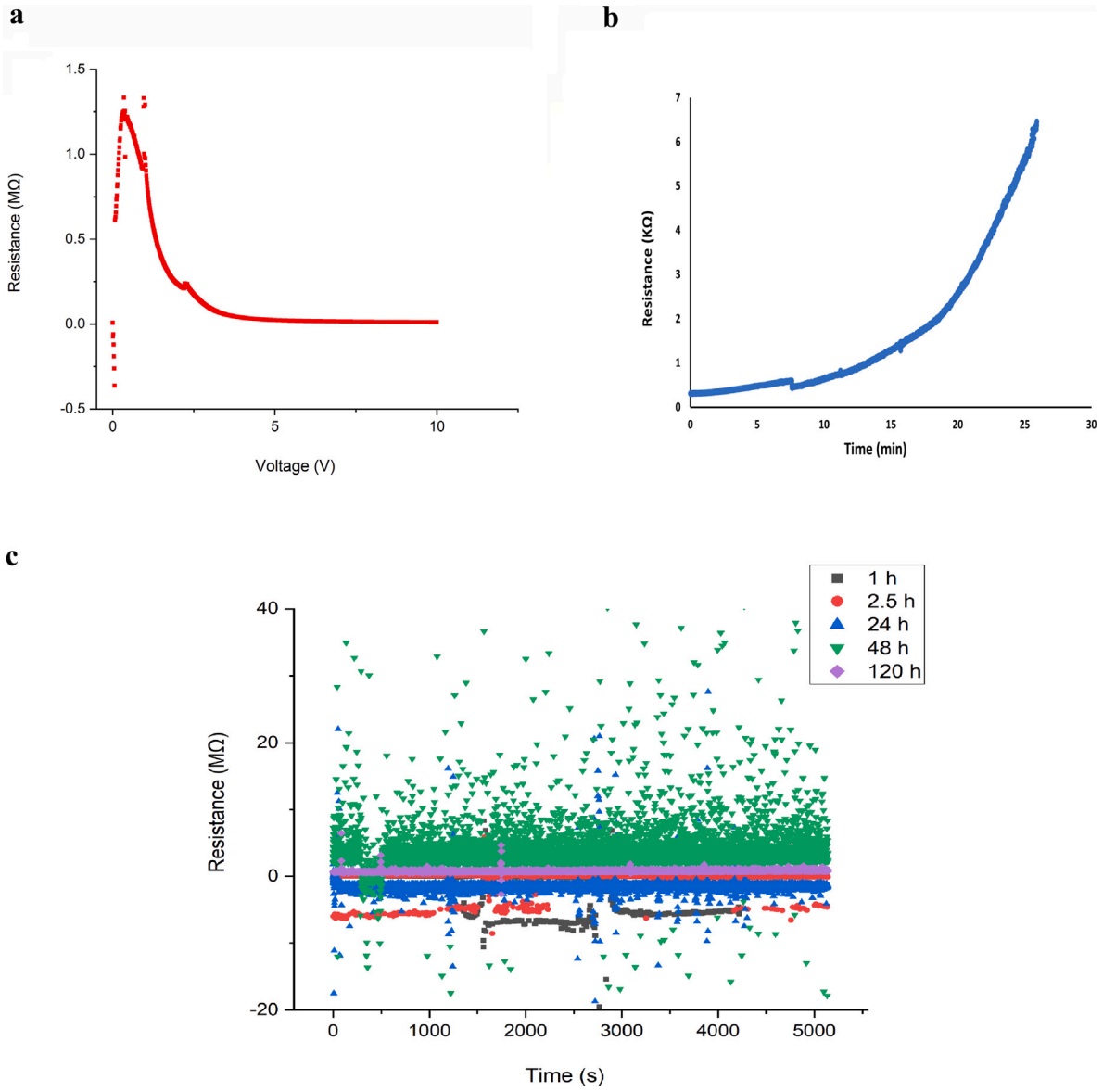

Fig. 8. Implementation of memory: (a) Resistance of the colloid before stimulation, (b) Resistance of the colloid with stimulation till 10 V, (c) Resistance of colloid after different hours.

This phenomenon can be utilized to prototype memory devices in liquid phase robots and computers, as well as to implement synaptic devices in liquid phase neuromorphic circuits. Future research directions could include the development of protocols for simulating the formation of multiple non-intersecting conductive pathways in a spherical volume of a colloid. In liquid robots and computers, these pathways would serve as information superhighways.

CRediT authorship contribution statement

Noushin Raeisi Kheirabadi: Designed the experiments, Conducted the experiments, Discussed and analysed the results, Drafted, reviewed, edited and approved the manuscript. **Alessandro Chiolerio:** Proposed the idea and general approach, Designed the experiments, Discussed and analysed the results, Drafted, reviewed, edited and approved the manuscript. **Neil Phillips:** Discussed and analysed the results, Drafted, reviewed, edited and approved the manuscript. **Andrew Adamatzky:** Proposed the idea and general approach, Designed the experiments, Discussed and analysed the results, Drafted, reviewed, edited and approved the manuscript.

Declaration of competing interest

The authors declare that they have no known competing financial interests or personal relationships that could have appeared to influence the work reported in this paper.

Data availability

Data will be made available on request.

Acknowledgements

The authors are grateful to David Patton for performing FESEM characterization, Paul Bowdler for his help to use the UV–Visible spectroscopy device, and Michal Wagner or his assistance in using the UV–Visible spectroscopy device.

This project has received funding from the European Union's Horizon 2020 research and innovation programme FET OPEN "Challenging current thinking" under grant agreement No 964388.

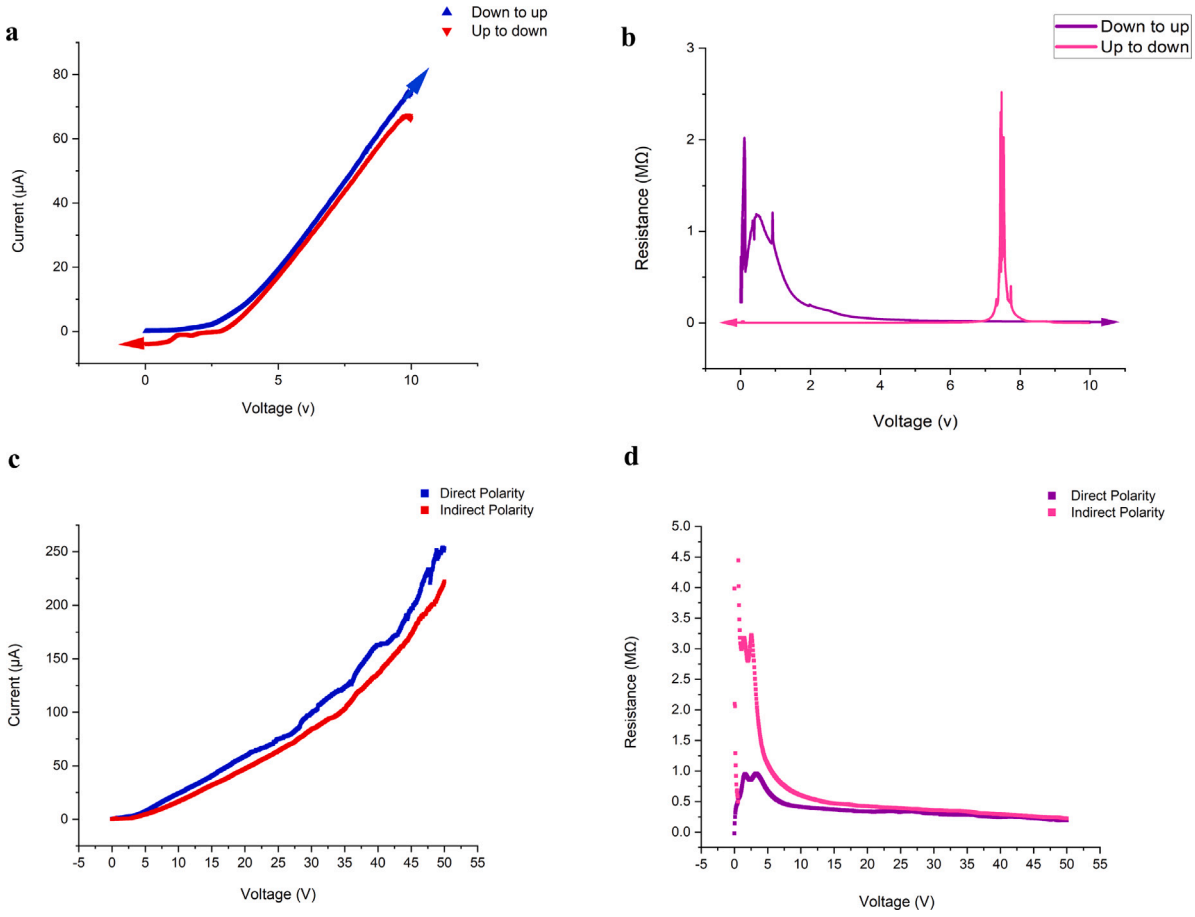

Fig. 9. (a) Current diagram and (b) Resistance diagram of colloid after DC stimulation from 0 V to 10 V and then from 10 V to 0 V. (c) Current diagram of colloid after 50 V DC stimulation with direct and indirect polarity, (d) Resistance diagram of colloid after 50 V DC stimulation with direct and indirect polarity.

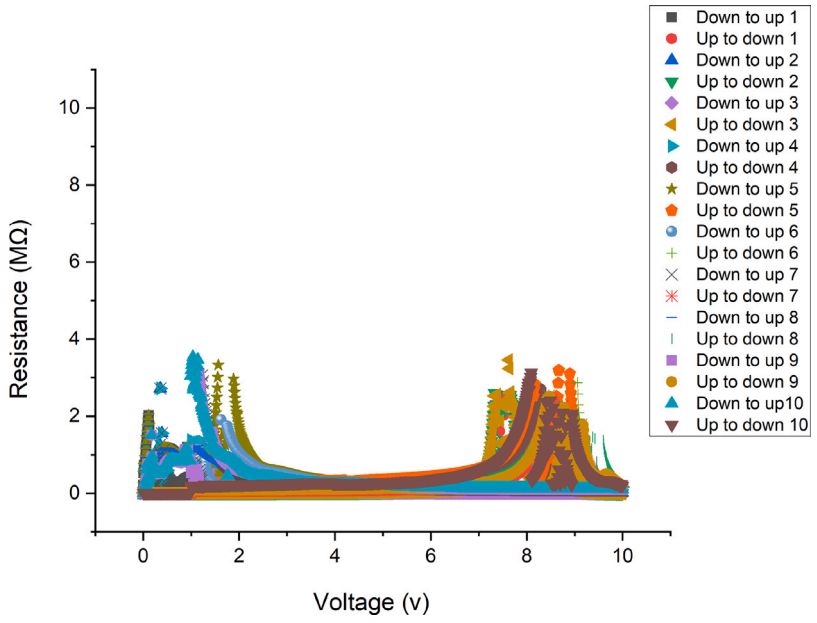

Fig. 10. Multiple cycles of direct-inverse stimulation to evaluate durability of the colloidal device.

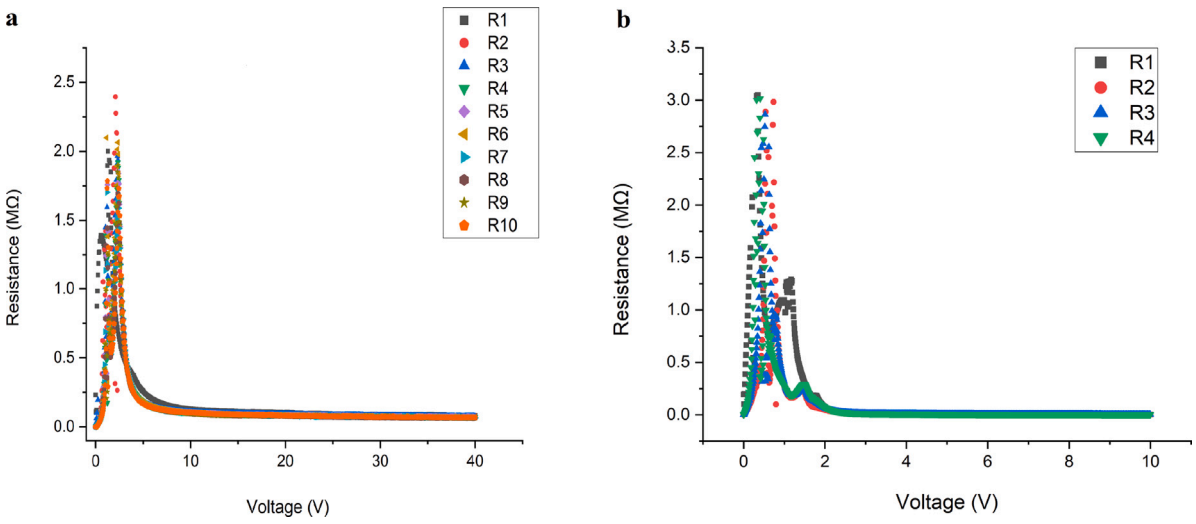

Fig. 11. (a) Repeated measurement resistance of colloid with DC stimulation in the ambient atmosphere. (b) Repeated measurement resistance of colloid with DC stimulation in the Nitrogen atmosphere and at 12 °C.

References

[1] Andrew Adamatzky, Handbook of Unconventional Computing, World Scientific, 2021.

[2] Lilia S. Xie, Grigorii Skorupskii, Mircea Dincă, Electrically conductive metal–organic frameworks, Chem. Rev. 120 (16) (2020) 8536–8580, PMID: 32275412.

[3] Marco Sangermano, Alessandro Chiolerio, Giulio Marti, Paola Martino, UV-cured acrylic conductive inks for microelectronic devices, Macromol. Mater. Eng. 298 (2013) 607–611.

[4] M. Sumita, S. Asai, N. Miyadera, E. Jojima, K. Miyasaka, Electrical conductivity of carbon black filled ethylene-vinyl acetate copolymer as a function of vinyl acetate content, Colloid Polym. Sci. 264 (3) (1986) 212–217.

[5] Bernhard Wessling, Electrical conductivity in heterogeneous polymer systems. V (1): Further experimental evidence for a phase transition at the critical volume concentration, Polym. Eng. Sci. 31 (16) (1991) 1200–1206.

[6] Masao Sumita, Hibeki Abe, Hiroyuki Kayaki, Keizo Miyasaka, Effect of melt viscosity and surface tension of polymers on the percolation threshold of conductive-particle-filled polymeric composites, J. Macromol. Sci.—Phys. 25 (1–2) (1986) 171–184.

[7] Dietrich Stauffer, Scaling theory of percolation clusters, Phys. Rep. 54 (1) (1979) 1–74.

[8] Cheng Zhang, Ping Wang, Chun-an Ma, Guozhang Wu, Masao Sumita, Temperature and time dependence of conductive network formation: dynamic percolation and percolation time, Polymer 47 (1) (2006) 466–473.

[9] C. Zhang, J.F. Sheng, C.A. Ma, M. Sumita, Electrical and damping behaviors of CPE/BaTiO3/VGCF composites, Mater. Lett. 59 (28) (2005) 3648–3651.

[10] Jaime C. Grunlan, William W. Gerberich, Lorraine F. Francis, Lowering the percolation threshold of conductive composites using particulate polymer microstructure, J. Appl. Polym. Sci. 80 (4) (2001) 692–705.

[11] Micaela Castellino, Alessandro Chiolerio, Muhammad Imran Shahzad, Pravin Vithal Jagdale, Alberto Tagliaferro, Electrical conductivity phenomena in an epoxy resin–carbon-based materials composite, Composites: A 61 (2014) 108–114.

[12] Keizo Miyasaka, Kiyosi Watanabe, Eiichiro Jojima, Hiromi Aida, Masao Sumita, Kinzo Ishikawa, Electrical conductivity of carbon-polymer composites as a function of carbon content, J. Mater. Sci. 17 (6) (1982) 1610–1616.

[13] Xianhu Liu, Yamin Pan, Xiaoqiong Hao, Kun Dai, Dirk W Schubert, The role of conductive pathways in the conductivity and rheological behavior of poly (methyl methacrylate)–graphite composites, J. Appl. Polym. Sci. 133 (32) (2016).

[14] Wenlin Li, Yaqiong Zhang, Jingjing Yang, Jun Zhang, Yanhua Niu, Zhigang Wang, Thermal annealing induced enhancements of electrical conductivities and mechanism for multiwalled carbon nanotubes filled poly (ethylene-co-hexene) composites, ACS Appl. Mater. Interfaces 4 (12) (2012) 6468–6478.

[15] Samuele Porro, Francesca Risplendi, Giancarlo Cicero, Katarzyna Bejtka, Gianluca Milano, Paola Rivolo, Alladin Jasmin, Alessandro Chiolerio, Candido Fabrizio Pirri, Carlo Ricciardi, Multiple resistive switching in core–shell ZnO nanowires exhibiting tunable surface states, J. Mater. Chem. C 5 (2017) 10517–10523.

[16] Alessandro Chiolerio, Ignazio Roppolo, Katarzyna Bejtka, Abil Asvarov, Candido Fabrizio Pirri, Resistive hysteresis in flexible nanocomposites and colloidal suspensions: interfacial coupling mechanism unveiled, RSC Adv. 6 (2016) 56661–56667.

[17] Yang Zhang, Yongsheng Chen, Paul Westerhoff, Kiril Hristovski, John C Crittenden, Stability of commercial metal oxide nanoparticles in water, Water Res. 42 (8–9) (2008) 2204–2212.

[18] Alessandro Chiolerio, Marco B. Quadrelli, Smart fluid systems: the advent of autonomous liquid robotics, Adv. Sci. 4 (7) (2017) 1700036.

[19] Alessandro Chiolerio, Liquid cybernetic systems: The fourth-order cybernetics, Adv. Intell. Syst. 2 (12) (2020) 2000120.

[20] Marvin L. Cohen, The theory of real materials, Annu. Rev. Mater. Sci. 30 (1) (2000) 1–26.

[21] L Dong, YC Liu, YH Tong, ZY Xiao, JY Zhang, YM Lu, DZ Shen, XW Fan, Preparation of ZnO colloids by aggregation of the nanocrystal subunits, J. Colloid Interface Sci. 283 (2) (2005) 380–384.

[22] Marco Laurenti, Alessio Verna, Alessandro Chiolerio, Evidence of negative capacitance in piezoelectric ZnO thin films sputtered on interdigital electrodes, ACS Appl. Mater. Interfaces 7 (2015) 24470–24479.

[23] Woojin Lee, Jiwoo Yeop, Jungwoo Heo, Yung Jin Yoon, Song Yi Park, Jaeki Jeong, Yun Seop Shin, Jae Won Kim, Na Gyeong An, Dong Suk Kim, et al., High colloidal stability ZnO nanoparticles independent on solvent polarity and their application in polymer solar cells, Sci. Rep. 10 (1) (2020) 1–10.

[24] E. Marín, A. Calderón, D. Díaz, Thermal characterization of ZnO-DMSO (dimethyl sulfoxide) colloidal dispersions using the inverse photopyroelectric technique, Anal. Sci. 25 (5) (2009) 705–709.

[25] Hao Tang, Xinfang Chen, Aoqing Tang, Yunxia Luo, Studies on the electrical conductivity of carbon black filled polymers, J. Appl. Polym. Sci. 59 (3) (1996) 383–387.

[26] Harvey Scher, Richard Zallen, Critical density in percolation processes, J. Chem. Phys. 53 (9) (1970) 3759–3761.

[27] Scott Kirkpatrick, Percolation and conduction, Rev. Modern Phys. 45 (4) (1973) 574.

[28] Shameem Akhter, Jason Roberts, Multi-Core Programming, Vol. 33, Intel press Hillsboro, Oregon, 2006.

[29] Hong Han, Haiyang Yu, Huanhuan Wei, Jiangdong Gong, Wentao Xu, Recent progress in three-terminal artificial synapses: from device to system, Small 15 (32) (2019) 1900695.

[30] Yoeri van De Burgt, Armantas Melianas, Scott Tom Keene, George Malliaras, Alberto Salleo, Organic electronics for neuromorphic computing, Nat. Electron. 1 (7) (2018) 386–397.

[31] Noushin Raeisi Kheirabadi, Alessandro Chiolerio, Konrad Szaciłowski, Andrew Adamatzky, Neuromorphic liquids, colloids, and gels: a review, ChemPhysChem 24 (1) (2023) e202200390.

[32] K. Anand, Sibi Varghese, A. Krishnamoorthy, Role of surfactants on the stability of nano-zinc oxide dispersions, Part. Sci. Technol. 35 (2017) 67–70.

[33] Manoj Pudukudy, Zahira Yaakob, Facile synthesis of quasi spherical ZnO nanoparticles with excellent photocatalytic activity, J. Clust. Sci. 26 (4) (2015) 1187–1201.

[34] A Jagannatha Reddy, MK Kokila, H Nagabhushana, JL Rao, C Shivakumara, BM Nagabhushana, RPS Chakradhar, Combustion synthesis, characterization and Raman studies of ZnO nanopowders, Spectrochim. Acta A 81 (1) (2011) 53–58.

[35] Jian-Hui Sun, Shu-Ying Dong, Jing-Lan Feng, Xiao-Jing Yin, Xiao-Chuan Zhao, Enhanced sunlight photocatalytic performance of Sn-doped ZnO for Methylene Blue degradation, J. Mol. Catal. A: Chem. 335 (1–2) (2011) 145–150.

[36] Sotirios Baskoutas, Gabriel Bester, Conventional optics from unconventional electronics in ZnO quantum dots, J. Phys. Chem. C 114 (20) (2010) 9301–9307.

[37] Sotirios Baskoutas, Gabriel Bester, Transition in the optical emission polarization of ZnO nanorods, J. Phys. Chem. C 115 (32) (2011) 15862–15867.
[38] Pei-Jia Lu, Wei-En Fu, Shou-Chieh Huang, Chun-Yen Lin, Mei-Lin Ho, Yu-Pen Chen, Hwei-Fang Cheng, Methodology for sample preparation and size measurement of commercial ZnO nanoparticles, J. Food Drug Anal. 26 (2) (2018) 628–636.
[39] Mohd Omar Fatehah, Hamidi Abdul Aziz, Serge Stoll, Stability of ZnO nanoparticles in solution. Influence of pH, dissolution, aggregation and disaggregation effects, J. Colloid Sci. Biotechnol. 3 (1) (2014) 75–84.

Noushin Raeisi Kheirabadi is a Research Fellow working on learning and computing in colloids within the framework of the COgITOR project. She got her Ph.D. in Nanotechnology at Department of Materials Engineering, Isfahan University of Technology (IUT), Iran. She started experimental research on learning in colloidal systems, in the framework of European Innovation Council FETOpen project COgITOR: Colloid Cybernetic Systems at the University of the West of England (UWE). Her research focuses on learning and computing in colloidal frameworks, and triboelectric nanogenerators. Her research interests include Learning in Materials, Nanomaterials and Nano-colloids, Energy harvesting, Two-dimensional Nanostructures, Triboelectric Nanogenerators.

Professor Alessandro Chiolerio obtained his Ph.D. from the Physics Department of Politecnico di Torino in 2009 where he exploited quantum confinement in metals to perform information processing via the electron spin channel. In the following years, he studied transport properties of nanocomposite materials, exploring the conditions for percolation and the occurrence of resistive switching. He visited several institutes, such as NASA's Jet Propulsion Laboratory (Pasadena, USA), the Max Planck Institute (Halle, DE) and the University of the West of England (Bristol, UK) where he is visiting professor. His research field encompasses liquid state cybernetic systems, holonomic information processing, complex living systems. He is now at the Bioinspired Soft Robotics group of Istituto Italiano di Tecnologia, Genova (Italy). Author of more than 130 scientific articles, he has raised over € 10 million in competitive funding and private capital.

Dr. Neil Phillips is a researcher at Faculty of Environment and Technology, University of the West of England, UK, with a focus on unconventional computing. He is passionate about discovering unconventional solutions to overcome enduring technical challenges. His research interests include: bio-computing, biomimicry, liquid marbles, Marimo, contactless cell mapping, bio-reactors, bio-sensing, slime mould, fungi, and high temperature superconductors.

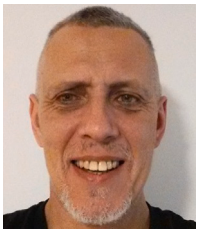

Andrew Adamatzky is Professor of Unconventional Computing and Director of the Unconventional Computing Laboratory, Department of Computer Science, University of the West of England, Bristol, UK. He does research in molecular computing, reaction–diffusion computing, collision-based computing, cellular automata, slime mould computing, massive parallel computation, applied mathematics, complexity, nature-inspired optimization, collective intelligence and robotics, bionics, computational psychology, non-linear science, novel hardware, and future and emergent computation. He has authored seven books, mostly notable are 'Reaction-Diffusion Computing', 'Dynamics of Crow Minds', and 'Physarum Machines', and has edited 22 books in computing, most notable are 'Collision Based Computing', 'Game of Life Cellular Automata', and 'Memristor Networks'. He has also produced a series of influential artworks published in the atlas 'Silence of Slime Mould'. He is Founding Editor-in-Chief of 'J of Cellular Automata' and 'J of Unconventional Computing' and Editor-in-Chief of 'J Parallel, Emergent, Distributed Systems' and 'Parallel Processing Letters'.